Journal of Human Evolution 109 (2017) 70–78

Contents lists available at ScienceDirect

Journal of Human Evolution

journal homepage: www.elsevier.com/locate/jhevol

News and Views

Further human fossils from the Middle Stone Age deposits of Die Kelders Cave 1, Western Cape Province, South Africa

Frederick E. Grine [a, b, *], Curtis W. Marean [c, d], J. Tyler Faith [e], Wendy Black [f], Carrie S. Mongle [g], Erik Trinkaus [h], Stephan G. le Roux [i], Anton du Plessis [i]

[a] Department of Anthropology, Stony Brook University, Stony Brook, NY 11794-4364, USA
[b] Department of Anatomical Sciences, Stony Brook University, Stony Brook, NY 11794-4364, USA
[c] Institute of Human Origins, School of Human Evolution and Social Change, Arizona State University, Tempe, AZ 85287-2402, USA
[d] Centre for Coastal Palaeoscience, Nelson Mandela Metropolitan University, Port Elizabeth, South Africa
[e] School of Social Science, The University of Queensland, Brisbane, QLD 4072, Australia
[f] Pre-Colonial Archaeology Unit, Social History Collections, Iziko Museums of South Africa, Cape Town, South Africa
[g] Interdepartmental Doctoral Program in Anthropological Sciences, Stony Brook University, Stony Brook, NY 11794, USA
[h] Department of Anthropology, Washington University, St. Louis, MO 63130, USA
[i] CT Scanner Unit, Central Analytical Facilities of Stellenbosch University, Stellenbosch 7602, South Africa

ARTICLE INFO

Article history:
Received 27 January 2017
Accepted 22 May 2017
Available online 29 June 2017

Keywords:
Deciduous
Incisor
Molar
Distal phalanx

1. Introduction

Southern African Middle Stone Age (MSA) sites that date to Marine Isotope Stages (MIS) 6–3 have featured prominently in discussions about the emergence of modern human behavior and morphology. In large measure, these sites have been emphasized because of the archaeological debris that they contain (e.g., Deacon, 1992, 2001; Klein, 2001; Henshilwood et al., 2002, 2011; Henshilwood and Marean, 2003; Klein et al., 2004; Marean et al., 2007; Conard, 2008; Wurz, 2008; Wadley et al., 2009; Texier et al., 2010; Vanhaeren et al., 2013; Marean, 2015). Although 15 sites from within this temporal span preserve human remains, these are largely in the form of isolated teeth and small cranial and/or postcranial fragments (Table 1) (Grine, 2016). Klasies River Main Site is by far the richest among them, with nearly 50 human fossils spread across three stratigraphic members that span some 40,000 years (Grine et al., 2017). Die Kelders Cave 1 is the second richest site, having yielded 27 specimens that have been published to date (Grine, 2000). In view of the relative paucity of human remains from the MSA of southern and, indeed, sub-Saharan Africa (Grine, 2016), every discovery is worthy of documentation. We here report on three additional human specimens from the MSA deposits of Die Kelders Cave 1.

The site of Die Kelders (34°32′S, 19°22′E) comprises a pair of contiguous caves, Die Kelders Cave 1 (DK1) and Die Kelders Cave 2 (DK2), located near sea level on the southern coast of the Western Cape Province. Excavations by F.R. Schweitzer between 1969 and 1973 revealed a thick series of MSA deposits in DK1 (Schweitzer, 1970, 1979; Tankard and Schweitzer, 1974, 1976; Tankard, 1976). These were recognized as comprising 12 layers (numbered 4–15 from top to bottom). Schweitzer's work resulted in the recovery of 13 human teeth (Table 2). These specimens have been described by Grine et al. (1991) and in Avery et al. (1997). Excavations between 1992 and 1995 by a team from Stony Brook University (F.E. Grine and C.W. Marean), Stanford University (R.G. Klein) and the Iziko South African Museum (G. Avery) recovered an additional 14 human fossils (Marean et al., 2000). These specimens have been described in Avery et al. (1997) and by Grine (1998, 2000). Most of the human specimens from the MSA horizons of DK1 that have been published comprise isolated teeth (Table 2). While they derive from the uppermost (Layer 4) through the lowermost (Layer 15) horizons, nearly two-thirds of the sample derives from Layer 6, which has also yielded most of the larger mammalian (e.g., bovid) fauna (Klein and Cruz-Uribe, 2000). The entire assemblage appears to have been deposited over a comparatively short time interval (ca. 10,000 years) between about 75–64 kya or 70–60 kya as

* Corresponding author.
E-mail addresses: frederick.grine@stonybrook.edu (F.E. Grine), Curtis.Marean@asu.edu (C.W. Marean), j.faith@uq.edu.au (J.T. Faith), wblack@iziko.org.za (W. Black), carrie.mongle@stonybrook.edu (C.S. Mongle), trinkaus@wustl.edu (E. Trinkaus), lerouxsg@sun.ac.za (S.G. le Roux), anton2@sun.ac.za (A. du Plessis).

http://dx.doi.org/10.1016/j.jhevol.2017.05.009

Table 1
Hominin-bearing South African MSA sites dating from MIS 6 through MIS 3.

MIS	Site	Site age (ka)	Hominin remains
6–3	Border Cave	170–56	Postcranial fragments
5e	Blind River	124–112	Femur
5e-4	Klasies River	115–58	Multiple cranial, mandibular and postcranial fragments
5e-5a	Sea Harvest	110–71	Manual distal phalanx; tooth
5c-3	Equus Cave	103–30	Eight teeth
6-5c	Pinnacle Point	162–90	Parietal; tooth
5c-5a	Blombos	102–70	Nine teeth
5c-3	Ysterfontein 1	130–50	Three teeth
5c-3	Witkrans	100–50	Three teeth
5a-4	Plovers Lake	89–62	Postcranial fragments
4	Die Kelders Cave 1	74–59	24 teeth; mandibular fragment; two phalanges
4	Klipdrift Shelter	72–52	Tooth
3	Sibudu	77–38	Phalanx; distal fibula
3	Diepkloof	61–48	Two toe bones; one tooth
3	Hofmeyr	36	Cranium

Table 2
Previously described human remains from the MSA of Die Kelders Cave 1.

Specimen	Element	Layer	Grid co-ordinate	Excavation
AP 6245	Rdi^2	4	F-5[a]	1969–1973
AP 6244	Rdm^2	4	F-5[a]	1969–1973
AP 6264	LP^4	4/5	E-9	1993
AP 6242	RM_1	6	G-4[a]	1969–1973
AP 6243	Rdm^2	6	G-4[a]	1969–1973
AP 6246	Ldm_1	6	G-4[a]	1969–1973
AP 6247	Ld_c	6	G-4[a]	1969–1973
AP 6248	Rdi_2	6	D-5[a]	1969–1973
AP 6255	Rd^c	6	C-6[b]	1969–1973
AP 6256	Ld_c	6	C-6[b]	1969–1973
AP 6257	Rdm^2	6	F-5[b]	1969–1973
AP 6267	manual phalanx	6	E-8	1993
AP 6275	LI^1	6	E-8	1995
AP 6276	mandible with I_1	6	F-12	1995
AP 6277	LM_1	6	H-12	1995
AP 6280	$R\underline{C}$	6	G-10	1995
AP 6281	RP^4	6	E-11	1995
AP 6282	RM_2	6	E-11	1995
AP 6288	Ldi_2	6	G-8	1995
AP 6289	manual phalanx	6	G-11	1995
AP 6290	Ldi_1	6	E-11	1995
AP 6291	Ldm_1	8	E-2	1995
AP 6278	Rdi^1	10	F-11	1995
AP 6258	LP^4	11	D-4[b]	1969–1973
AP 6250	Rd^c	14	D-5[a]	1969–1973
AP 6279	RP_4	14	E-6	1995
AP 6249	Rdi^1	15	H-4[a]	1969–1973

[a] Specimens listed in Grine et al. (1991: Table 4).
[b] Specimens listed in Avery et al. (1997: Table 5) employed Schweitzer's grid reference. That reference is one letter designation (i.e., 1 m) to the north of the co-ordinates established in 1992. The grid co-ordinates used in the present table correspond to the latter.

determined by electron spin resonance (Schwarcz and Rink, 2000) and luminescence methods (Feathers and Bush, 2000).

The vast majority of the human specimens represent children, and all may derive from sub-adult individuals. Thus, 15 are deciduous teeth, one is a mandibular fragment with an unerupted LI_1, and two are immature permanent tooth germs. The seven permanent teeth display minimal to moderate wear, suggesting that they come from adolescents or very young adults. The two manual middle phalanges do not preserve the proximal base; thus, their epiphyseal status cannot be determined. The assemblage represents a minimum of ten individuals (Grine, 1998).

Three further human specimens — a distal pollical phalanx, a mandibular deciduous lateral incisor, and a fragment of a deciduous mandibular molar — have been identified recently among the faunal remains recovered by Schweitzer's and the joint team's excavations in DK1 (Table 3). These specimens are described and illustrated here.

Table 3
Additional human remains from the MSA of Die Kelders Cave 1.

Specimen	Element	Layer	Grid co-ordinate	Excavation
SAM-AP 6402	Pollical phalanx	4	B-3	1969–1973
SAM-AP 6403	Rdi_2	6	E-6	1995
SAM-AP 6404	Rdm_2 fragment	15	E-4	1969–1973

The distal pollical phalanx (SAM-AP 6402) was excavated by Schweitzer; it derives from Layer 4. The deciduous incisor (SAM-AP 6403) was excavated by the joint team in 1995. It comes from Layer 6. The mandibular molar fragment (SAM-AP 6404) was also excavated by Schweitzer, and is from Layer 15.

These specimens were studied and measured under strong incident light at Iziko Museums of South Africa, and examined by nano-computed tomography (General Electric Nanotom S) at Stellenbosch University (du Plessis et al., 2016) at an accelerating voltage of 60 kV and at a voxel size of 0.01413 mm in the x, y and z axes. X-ray projection images were acquired in 2200 steps during a full rotation of the sample. At each step position, the first image was disregarded and the subsequent two images averaged to produce higher quality images than standard. A detector shift was activated to minimize ring artefacts.

2. Descriptions

2.1. Pollical distal phalanx (SAM-AP 6402)

SAM-AP 6402 is a very nearly complete pollical distal phalanx (Fig. 1). The long axis of the element (as determined by a line that runs from a point bisecting the proximal facets to the distal apex) is virtually perpendicular to the transverse axis of the proximal facet. It is, therefore, not possible to determine the side from which it derives by employing the observation that the long axis of the human pollical distal phalanx tends to exhibit slight ulnar (medial) deviation relative to its interphalangeal articular surface (Trinkaus et al., 2014). For descriptive purposes it is treated as being from the left hand. The lateral (radial) edge of the apical tuft is missing, but the bone is otherwise complete. The surface exhibits some pitting that suggests slight acid etching; this is more evident on the palmar than the dorsal surface. It is not possible to determine if the etching resulted from exposure to carnivore (e.g., hyena or leopard) gastric acids, or to low pH conditions in the DK1 deposits. The base is expanded, providing the greatest dorsopalmar (DP) and mediolateral (ML) dimensions. The proximal surface has two indistinctly separated depressions for articulation with the condyles of the proximal phalanx. The shaft narrows distally to about mid-length, where it begins to expand to the distal tuberosity.[1] The proximal palmar surface presents a large depression adjacent to the base for the arcing insertion of the flexor pollicis longus (FPL) tendon. Distal to the FPL depression, the palmar surface expands anteriorly, producing an ovoid cross-sectional outline to the shaft. The base is

[1] The expansion at the distal end of the human manual distal phalanx has been variously referred to as the ungual process (Stack, 1958), ungual tuberosity (Shrewsbury and Johnson, 1983), ungual tuft (Susman, 1998) and apical tuft (Susman and Creel, 1979; Mittra et al., 2007). However, because the name distal phalangeal tuberosity (tuberositas phalangis distalis) is recognized by Nomina Anatomica (International Anatomical Nomenclature Committee, 1989) and its successor, Terminologia Anatomica (Federative Committee on Anatomical Terminology, 1998), we follow Shrewsbury et al. (2003) and Niewoehner (2007) in employing this term.

Figure 1. Volumetric renderings of the SAM-AP 6402 pollical distal phalanx. Dorsal view (upper left); palmar view (upper right); proximal basal view (lower left); medial (ulnar) view (lower right).

dorsally canted relative to the long axis of the shaft and distal tuberosity.

The basal epiphysis is fully fused. Fusion usually occurs between ages 13 and 17 in recent humans (Flecker, 1932; Joseph, 1951; Pyle et al., 1971; So, 1997; Glisanz and Ratib, 2005; Cardoso and Severino, 2010). This bone therefore derives from a late adolescent or fully adult individual.

Seven standard measurements of the bone were recorded with calipers and confirmed using surfaces rendered from the nanoCT scans in Avizo v9.2.0 (Table 4).

The cortical bone is moderately thick along most of the shaft and apical tuft, but is thinner in the region of the FPL excavation and at the base. There is no indication of cortical thinning having resulted from the slight acidic erosion that seems to manifest on the external surface. Trabeculae are numerous, with more expansive medullary space in the center of the shaft than in the base (Fig. 2). A video of the outer surface (volumetric rendering) and serial longitudinal sectioning of the specimen is available as Supplementary Online Material (SOM) Video S1.

Supplementary Online Material related to this article can be found online at http://dx.doi.org/10.1016/j.jhevol.2017.05.009.

2.2. Mandibular right lateral deciduous incisor (SAM-AP 6403)

SAM-AP 6403 is a moderately worn Rdi_2 that preserves a short segment of a broken, resorptive root (Fig. 3). The crown is complete. Incisal wear has produced an elongate dentine exposure, with antemortem enamel chipping at the mesial and distal extremes of the labial incisal edge. The mesial chip is larger than the distal. There is a small mesial interproximal wear facet and a very faint distal contact facet. The labial surface is featureless, and evinces no hypoplasia. Lingually, there is no evidence of a mesial marginal ridge; the faint distal marginal ridge is delineated by an extremely shallow depression above the basal swelling. The basal swelling exhibits a slight distalward cant.

The crown measures 4.90 mm mesiodistally (MD) and 4.74 mm buccolingually (BL). It is likely that the pristine MD diameter would have been slightly greater – probably 5.1 mm.

The labial rim of the root exhibits a series of shallow scallops that almost certainly relate to resorptive activity. The lingual rim of the root is damaged. Resorption of the di_2 root to this extent suggests an ontogenetic age of about 5 years on the basis of recent human standards (Al Qahtani et al., 2010).

The crown and root preserve a large amount of calculus. This is most strongly developed along the labial and especially the mesial aspects of the tooth. The presence of calculus over some 1.5 mm of the cervical portion of the root is indicative of gingival recession and, concomitantly, a degree of gingivitis or perhaps periodontitis in this individual (Philstrom et al., 2005). Although the number of MSA human gnathic remains from sub-Saharan and especially southern Africa precludes a meaningful assessment of the incidence of periodontitis (particularly in juveniles), this has been amply documented for the Eurasian Middle Palaeolithic Neandertals (Lacy,

Table 4
Measurements of the SAM-AP 6402 pollical distal phalanx (mm).

Maximum proximodistal length	
L	21.02
Distal tuberosity dimensions	
DPT	2.76
MLT	8.30 est.[a]
Midshaft dimensions	
DPMS	4.60
MLMS	6.67
Base dimensions	
DPB	8.55
MLB	12.36

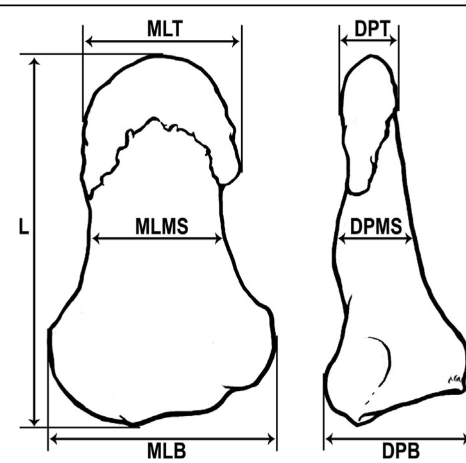

L = maximum proximodistal length; DPT = dorsopalmar distal tuberosity; MLT = mediolateral distal tuberosity; DPMS = dorsopalmar midshaft; MLMS = mediolateral midshaft; DPB = dorsopalmar base; MLB = mediolateral base.
The illustration of the measurement termini in schematic palmar and lateral views is adapted from Almécija et al. (2014: Fig. 2).
[a] MLT measures 7.56 mm as preserved. The estimated value (8.3 mm) was determined by doubling the distance from the lateral-most point of the preserved lateral edge to the midline.

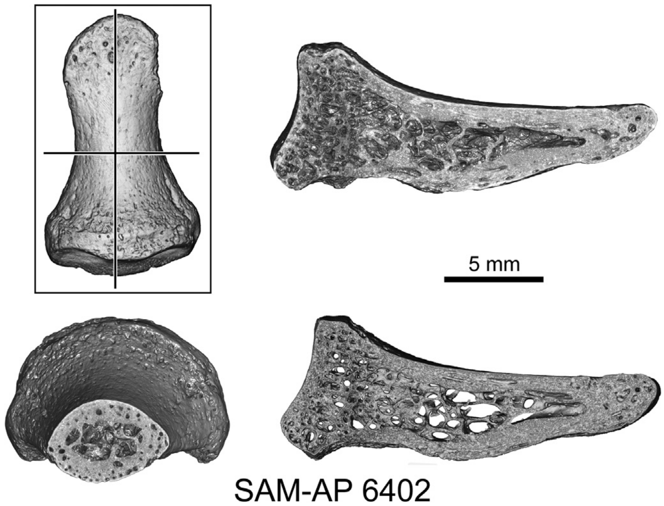

Figure 2. Nano-CT scan images through the midshaft of the SAM-AP 6402 pollical distal phalanx. Inset image shows locations of the CT sections. Transverse midshaft section (lower left); longitudinal midshaft section (upper and lower right).

2014; see references in Margvelashvili et al., 2016) and in Eurasian groups of Middle and Upper Palaeolithic modern humans (Lacy, 2014). Lacy (2014) reported that only 18.3% of the 120 Neandertal and modern human specimens in her sample displayed no evidence of periodontal inflammation, and that while the Neandertals exhibit a higher percentage of advanced cases, the Middle and Upper Paleolithic modern human groups do not differ significantly in their expression of periodontitis. Lacy concluded that, overall, the incidence of periodontal disease in the Eurasian Pleistocene is "much higher" than has been suggested heretofore. We would note that among the seven adult human mandibles or maxillae from Klasies River Main site (Grine et al., 2017), only the aged KRM 41815 (SAM-AP 6222) jaw has clear evidence of periodontal disease.

A video of the outer surface (volumetric rendering) of this tooth is available as Supplementary Online Material (SOM) Video S2.

Supplementary Online Material related to this article can be found online at http://dx.doi.org/10.1016/j.jhevol.2017.05.009.

This tooth is very similar to the SAM-AP 6288 Ldi$_2$ described by Grine (1998). The two crowns are of similar size (see below); both display a faint basal prominence that is skewed distally and a weak distal marginal ridge, and both lack a mesial marginal ridge. Neither displays labial hypoplasia, and in both the scalloped root edge is indicative of a similar state of resorption, with an estimated ontogenetic age of ca. 5 years. Moreover, both display dental calculus deposits around the cervical margin of the crown. These two teeth derive from Layer 6, and were found within two meters of one

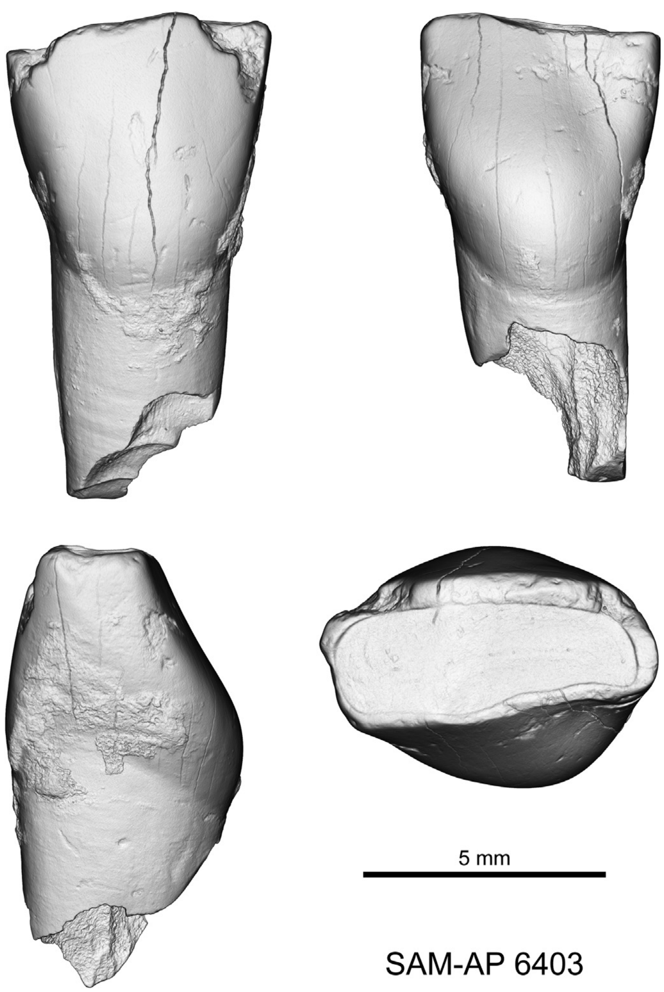

Figure 3. Volumetric renderings of the SAM-AP 6403 mandibular right deciduous lateral incisor. Labial view (upper left); lingual view (upper right); mesial view (lower left) incisal view (lower right).

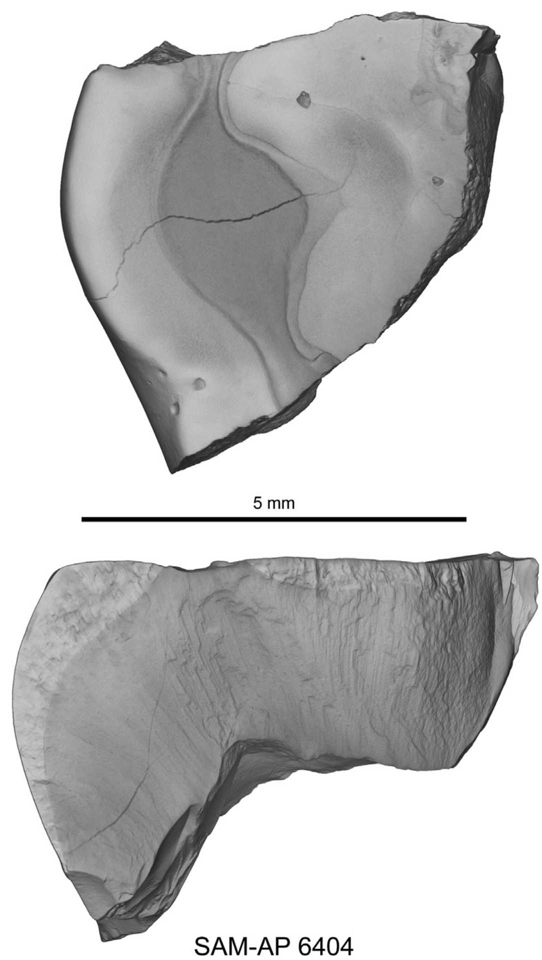

Figure 4. Volumetric renderings of the SAM-AP 6404 mandibular right deciduous second molar. Occlusal view, with buccal to the left and distal to the top (above); mesial view with buccal to the left (below).

another. Therefore, it is very likely that these two deciduous lateral incisors are antimeres. The SAM-AP 6288 Ldi_2 may derive from the same individual as the SAM-AP 6290 Ldi_1 (Grine, 1998).

2.3. Mandibular deciduous molar fragment (SAM-AP 6404)

SAM-AP 6404 is a small fragment of a moderately worn crown (Fig. 4). The fragment is interpreted here as preserving the buccal enamel wall and much of the worn hypoconid of a mandibular right molar crown. According to this interpretation, the hypoconid enamel is worn flat with a large dentine patch exposed in relation to the cusp tip. This patch is connected by a narrow isthmus of dentine to the protoconid exposure and a very narrow isthmus to the hypoconulid exposure. The fragment measures 6.11 mm at its greatest BL extent, and the buccal enamel wall measures 5.45 mm MD.

The enamel exposed on the mesial face is 0.97 mm thick when measured from the highest preserved buccal point along a straight line perpendicular to the enamel-dentine junction (EDJ). A value of 0.99 mm is obtained from a BL section of the enamel recorded through the middle of the hypoconid dentine exposure. Although it is not possible to determine the precise location of this measurement in relation to the pristine (unworn) cuspal architecture, it is probably situated between measurements “LTB” and “k” of Grine (2005). Measurement “LTB” is defined by a point on the EDJ 1.0 mm from the tip of the dentine horn. As such, a horizontal plane through it will cut through the dentine of the cusp apex and through the occlusal enamel on the lingual side of the cusp tip. Measurement “k” is recorded at a more cervical level, being coincident with a horizontal plane that passes through the lowest point of the EDJ between the buccal and lingual cusps. As such, a horizontal plane through the outer enamel terminus of this measurement will pass close to the bottom of the occlusal enamel on the lingual side of the buccal cusp. Linear enamel thickness measurement “LTB” will likely be somewhat greater than measurement “k” on any given molar. In view of the very thin layer of enamel that is preserved occlusally on the lingual side of the buccal cusp of SAM-AP 6404 (Fig. 4), it is likely that the enamel thickness measurements (average = 0.98 mm) are recorded closer to measurement “k” than measurement “LTB.”

The enamel thickness value of 0.98 mm recorded for SAM-AP 6404 is compared in Table 5 with the “k” and “LTB” values recorded by Grine (2005) for the dm_2 and mandibular permanent molars of a mixed sex population sample of recent humans. The SAM-AP 6404 value is clearly within the range of the values for measurement “k” of the dm_2 and closer to the deciduous linear averages than to the averages or observed ranges for any of the permanent molars. We therefore regard SAM-AP 6404 as most likely deriving from a Rdm_2.

Table 5
Buccal linear enamel thickness of SAM-AP 6404 compared with measurements though buccal protoconid enamel of recent human mandibular molars.

	n	x̄	SD	Obs. range
SAM-AP 6404		**0.98**		**0.97–0.99**
Measurement LTB				
dm2	10	1.13	0.08	1.00–1.30
M1	10	1.69	0.15	1.30–1.80
M2	10	1.88	0.19	1.60–2.20
M3	10	1.94	0.22	1.60–2.30
Measurement k				
dm2	10	0.98	0.15	0.80–1.20
M1	10	1.69	0.19	1.30–1.90
M2	10	1.69	0.29	1.00–2.00
M3	10	1.54	0.45	1.00–2.20

Data from Grine (2005: Table 3).

3. Comparisons

3.1. Pollical distal phalanx size and shape

The dimensions recorded for SAM-AP 6402 are compared with those for a number of recent human samples, a sample of early modern humans from the Middle – Upper Paleolithic of Eurasia and a sample of Neandertals in Table 6. The DK1 values are smaller than the corresponding means for the early modern sample and notably smaller than the Neandertal sample means.

The DK1 values also fall below the corresponding means for recent human samples for all measurements save for length and the DP depth of the base. The length of SAM-AP 6402 is slightly above the Khoesan sample mean, and its base is deeper than the averages recorded for all of the recent human samples save one from Europe. Nevertheless, in all instances, the dimensions of the DK1 phalanx fall within the observed ranges and within 1 or 2 SD of all of these recent human sample means. While the surface of SAM-AP 6402 appears to have been lightly etched by acid, this is unlikely to account for its comparatively small size.

By comparison with the Holocene Khoesan, the base of the DK1 phalanx is relatively deep but narrow in relation to its length (Fig. 5).

Table 6
Comparative pollical distal phalanx dimensions.

Dimension	Population	*n*	Mean	SD	Obs. range	Reference source
L	**SAM-AP 6402**		**21.02**			
	LSA Khoesan[a]	23	20.56	1.98	17.3–25.3	This study
	South Asian (India)	25	22.32	1.74	19.1–26.0	Almécija et al. (2014)
	Native American[b]	26	23.43	1.75	20.5–25.4	S. Smith (pers. comm.)
	African American[c]	80	25.31	2.11	21.3–30.4	S. Smith (pers. comm.)
	European[d]	80	23.01	1.95	18.5–27.6	S. Smith (pers. comm.)
	Early Modern[e]	19	22.57	2.24	19.3–27.5	This study
	Neandertal[f]	12	24.95	1.20	23.1–26.9	This study
DPT	**SAM-AP 6402**		**2.76**			
	LSA Khoesan	23	3.03	0.47	2.4–4.7	This study
	South Asian (India)	25	3.43	0.43	2.5–4.2	Almécija et al. (2014)
	Native American	26	3.88	0.47	3.1–4.8	S. Smith (pers. comm.)
	African American	80	3.87	0.47	3.0–4.9	S. Smith (pers. comm.)
	European	80	3.94	0.50	3.0–5.2	S. Smith (pers. comm.)
MLT	**SAM-AP 6402**		**8.30**			
	LSA Khoesan	23	8.61	0.78	7.0–10.5	This study
	South Asian (India)	25	9.28	1.12	7.1–11.1	Almécija et al. (2014)
	Native American	26	9.26	1.04	7.4–11.8	S. Smith (pers. comm.)

Table 6 (*continued*)

Dimension	Population	*n*	Mean	SD	Obs. range	Reference source
	Native American[g]	14	9.35	0.96	7.8–11.3	This study
	African American	80	10.15	1.15	7.9–13.2	S. Smith (pers. comm.)
	European	80	10.10	1.25	6.7–12.6	S. Smith (pers. comm.)
	European[h]	55	10.43	2.63	7.2–15.6	This study
	Early Modern	12	9.83	1.69	6.8–12.7	Trinkaus et al. (2014)
	Neandertal	15	12.40	1.32	9.5–14.5	Trinkaus et al. (2014)
DPMS	**SAM-AP 6402**		**4.60**			
	LSA Khoesan	23	4.86	0.67	3.4–6.7	This study
	South Asian (India)	25	4.47	0.56	3.4–5.3	Almécija et al. (2014)
	Native American	26	5.17	0.39	4.0–6.6	S. Smith (pers. comm.)
	Native American	14	4.92	4.92	4.1–5.4	This study
	African American	80	5.09	0.70	3.8–6.9	S. Smith (pers. comm.)
	European	80	5.19	0.70	3.9–6.7	S. Smith (pers. comm.)
	European	55	4.81	0.67	3.4–6.3	This study
	Early Modern	10	5.22	0.64	3.8–6.3	Trinkaus et al. (2014)
	Neandertal	15	5.02	0.65	3.6–6.6	Trinkaus et al. (2014)
MLMS	**SAM-AP 6402**		**6.67**			
	LSA Khoesan	23	7.13	0.48	6.2–7.9	This study
	South Asian (India)	25	7.44	0.79	6.0–8.7	Almécija et al. (2014)
	Native American	26	7.78	0.86	6.1–9.8	S. Smith (pers. comm.)
	Native American	14	8.01	0.72	6.9–9.2	This study
	African American	80	7.97	0.99	6.1–10.5	S. Smith (pers. comm.)
	European	80	7.94	0.91	5.7–9.7	S. Smith (pers. comm.)
	European	55	8.01	0.91	6.0–10.0	This study
	Early Modern	12	8.33	1.08	6.5–9.9	Trinkaus et al. (2014)
	Neandertal	15	9.62	0.87	7.5–11.0	Trinkaus et al. (2014)
DPB	**SAM-AP 6402**		**8.55**			
	LSA Khoesan	23	7.65	0.54	6.6–8.5	This study
	South Asian (India)	25	8.22	0.68	7.0–9.7	Almécija et al. (2014)
	Native American	26	8.52	0.51	7.4–9.6	S. Smith (pers. comm.)
	Native American	14	8.25	0.55	6.9–9.0	This study
	African American	80	8.65	0.76	7.3–10.4	S. Smith (pers. comm.)
	European	80	8.42	0.78	6.7–10.0	S. Smith (pers. comm.)
	European	55	8.75	0.88	6.9–10.3	This study
	Early Modern	9	9.22	0.79	8.0–10.2	Trinkaus et al. (2014)
	Neandertal	13	9.02	1.20	6.3–10.8	Trinkaus et al. (2014)
MLB	**SAM-AP 6402**		**12.36**			
	LSA Khoesan	23	13.21	0.90	11.3–15.1	This study
	South Asian (India)	25	14.03	1.09	12.0–16.3	Almécija et al. (2014)
	Native American	26	14.21	0.22	12.3–16.5	S. Smith (pers. comm.)
	African American	80	14.95	1.25	12.6–17.5	S. Smith (pers. comm.)
	European	80	14.53	1.27	11.9–17.5	S. Smith (pers. comm.)
	European	55	15.23	1.52	12.1–18.4	This study
	Native American	14	14.09	0.86	12.2–15.6	This study
	Early Modern	14	15.28	0.96	13.6–17.0	Trinkaus et al. (2014)
	Neandertal	12	16.20	1.29	13.2–18.3	Trinkaus et al. (2014)

L = maximum proximodistal length; DPT = dorsopalmar distal tuberosity; MLT = mediolateral distal tuberosity; DPMS = dorsopalmar midshaft; MLMS = mediolateral midshaft; DPB = dorsopalmar base; MLB = mediolateral base.

[a] The Later Stone Age Khoesan sample measured by one of us (WB) comprises radiocarbon dated specimens from the Northern Cape, Western Cape and Eastern Cape provinces of South Africa.

[b] The Native American sample comprises nine female and 17 male specimens from the Sully and Mobridge sites, as documented by Smith (2000).

[c] The African American sample comprises 40 female and 40 male specimens from the Terry collection, as documented by Smith (2000).

[d] The European sample comprises 40 female and 40 male specimens from the Terry (38 male; 27 female) and Huntington (two male; 13 female) Collections. This sample consists of both European and European American individuals.

[e] The early modern human sample measurements were either taken by one of us (ET) or derive from primary descriptions of the remains (Verneau, 1906; Matiegka, 1938; McCown and Keith, 1939; Crevecoeur, 2008); it comprises Middle and Upper Paleolithic specimens from the sites of Barma Grande, Caviglione, Dolní Věstonice, Grotte-des-Enfants, Nazlet Khater, Pataud, Předmostí, Qafzeh, Skhūl, Sunghir and Obłazowa.

[f] The Neandertal sample measurements were either taken by one of us (ET) or derive from a primary description of the remains (Crevecoeur, 2002); it comprises specimens from the sites of La Ferrassie, Kebara, Kiik-Koba, Krapina, Palomas, Regourdou, Saint-Césaire and Shanidar.

[g] The Native American sample measured by one of us (ET) derives from Pecos Pueblo, New Mexico, USA.

[h] The European sample comprises recent British individuals measured by Musgrave (1970) and Medieval Europeans from the site of Mistihalj, Montenegro measured by one of us (ET).

In order to evaluate potential shape differences between the DK1 phalanx and those comprising the Holocene Khoesan, Late Pleistocene early modern and Neandertal samples, six of the measurements (excluding the DP thickness of the distal tuberosity) were adjusted for size by dividing by their geometric mean (Jungers et al., 1995). A principal components analysis (PCA) was performed using the individual specimens for each sample in R v3.1.2 (R Core Team, 2014). The result (Fig. 6) clearly separates Neandertals from the early modern and Khoesan specimens along the first principal component (PC1), which describes 43.8% of the variance. The separation is related to the notably ML broad shafts and distal tuberosities of the Neandertal pollical distal phalanges in relation to those of modern humans (Musgrave, 1973; Trinkaus, 1983, 2006). While the presence of a distinct distal tuberosity may be

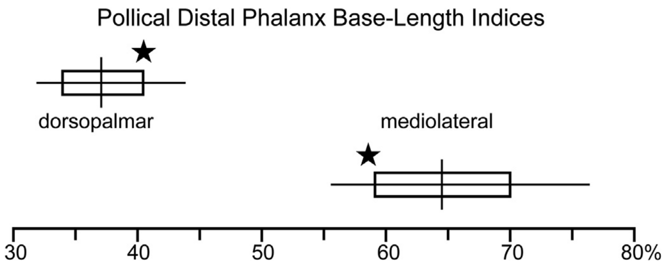

Figure 5. Dorsopalmar base/length and mediolateral base/length index values of SAM-AP 6402 (stars) compared with the corresponding mean, standard deviation and observed ranges for Holocene Later Stone Age Khoesan homologues.

plesiomorphic for *Homo* (Almécija et al., 2010), its expansion into a "mushroom-like" structure is best documented for the Neandertals and their immediate predecessors (Rosas, 1985; Lorenzo, 2007; Trinkaus, 2016). However, the polarity of this distal digital expansion is unclear, since the Early Pleistocene OH 7 and SK 5016 pollical distal phalanges have broad distal tuberosities (Napier, 1962; Susman, 1989), as does the *Homo naledi* homologue (Kivell et al., 2015).

The DK1 phalanx occupies a position at the margin of the Khoesan sample on PC1 owing to its relatively deep shaft and base. On the other hand, the DK1 bone occupies an intermediate position in relation to the Khoesan sample along the second principal component (PC2), which explains 23.2% of the variance. As such, SAM-AP 6402 is perhaps not unusual among Holocene Khoesan homologues, but can be distinguished morphometrically from Pleistocene Eurasian specimens. Indeed, the distal tuberosity (and

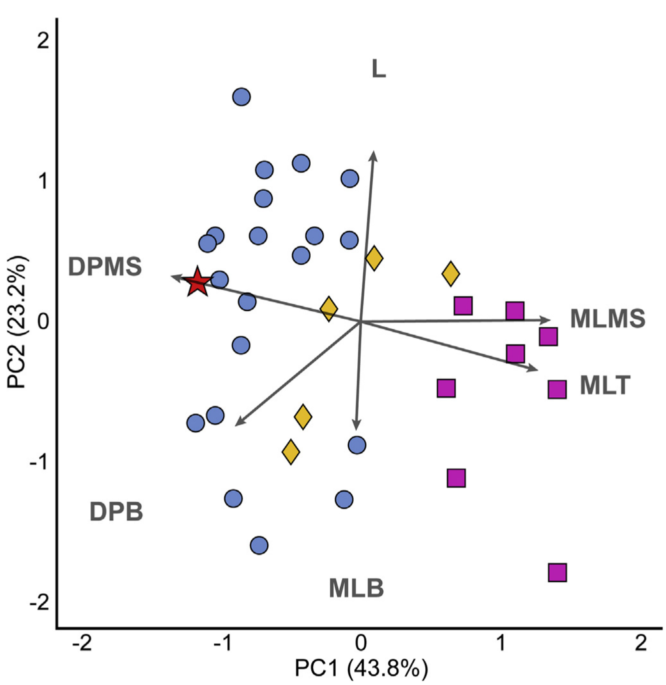

Figure 6. Principal components analysis of six linear dimensions of the SAM-AP 6402 (red star), Khoesan (blue circles), early modern (yellow diamonds) and Neandertal (purple squares) pollical distal phalanges. See Table 4 for explanation of the dimension abbreviations. The lengths of the arrows correspond to how heavily each dimension loads on a particular axis. The early modern sample comprises specimens from Qafzeh, Dolní Věstonice, Nazlet Khater, Obłazowa and Sunghir; the Neandertal sample comprises specimens from Kiik-Koba, Kebara, Krapina, Palomas, Saint-Césaire and Shanidar. (For interpretation of the references to colour in this figure legend, the reader is referred to the web version of this article.)

diaphysis) of SAM-AP 6402 is also relatively narrow, making it appear rather gracile in comparison to those of Middle and Upper Paleolithic modern humans (Crevecoeur, 2008; Trinkaus, 2016).

As noted above, the absence of distal ulnar deviation in the DK 1 phalanx is also unusual among Middle and Late Pleistocene homologues. Its ulnar angle ($\approx 0°$) is matched by the Early Pleistocene SK 5016 and occasional recent humans, but it is more than 2 SDs from samples of Middle Pleistocene *Homo* ($5.4° \pm 1.7°$, $n = 7$), Neandertals ($7.3° \pm 3.0°$, $n = 14$) and Middle/Upper Paleolithic modern humans ($2.8° \pm 1.3°$, $n = 8$).

3.2. Mandibular lateral deciduous incisor size and morphology

The MD and BL crown measurements recorded for the SAM-AP 6403 di_2 are compared with those recorded for recent human homologues in Table 7. As noted above, this crown is very similar to the SAM-AP 6288 di_2; both are somewhat smaller than the SAM-AP 6248 homologue that also derives from Layer 6.

The SAM-AP 6403 dimensions are larger than the corresponding means for the recent human samples, but in most instances these values fall within 1 or 2 SD of those sample means. While the Die Kelders teeth tend to be large by comparison with recent African homologues, they more closely approximate the plesiomorphic sizes of the Neandertal deciduous teeth.

Morphologically, the Die Kelders di_2s resemble the vast majority of recent southern African homologues in the lack of lingual shoveling and the absence of a basal lingual tubercle (Grine, 1986, 1990).

4. Discussion and conclusion

The new specimens from the MSA horizons of Die Kelders Cave 1 add to the meager and all too fragmentary human fossil sample from the Late Pleistocene of South Africa. The di_2 is very likely the antimere of a tooth described earlier (Grine, 1998). The pollical distal phalanx represents a late adolescent or fully adult individual, which contrasts with the subadult nature of most of the specimens from the site. It is the only manual distal phalanx known from DK1.

These specimens provide some additional evidence pertaining to the morphological attributes of these people. Overall, the phalanx is relatively small by comparison with recent and early modern specimens from Eurasia, although it tends to be a little longer and its base tends to be somewhat deeper than in the majority of Khoesan homologues. Overall, it is notably more similar to the Holocene Khoesan than to Late Pleistocene Eurasian early modern or to Neandertal pollical distal phalanges. It possesses thick cortical bone and a well-developed trabecular network. The deciduous incisor, on the other hand, like its antimere, tends to be relatively large by comparison with recent African homologues. In this regard, it is similar to some, but not all, of the other later Pleistocene specimens from southern African sites, such as Klasies River Mouth, Equus Cave, and Witkrans (Singer and Wymer, 1982; Grine and Klein, 1985; Rightmire and Deacon, 1991; McCrossin, 1992). This is perhaps not unexpected. Not only is large tooth size plesiomorphic but crown reduction has been documented from even more recent archaeological samples to living populations (Frayer, 1977; Chamla, 1980; Brace and Vizthum, 1984; Calcagno, 1986; Brace et al., 1987; Brace, 1995; Christensen, 1998; Kitagawa et al., 2002; Hill, 2004; Pinhasi et al., 2008; Pinhasi and Meiklejohn, 2011). However, some instances of temporal stasis or increase have been documented (Garn et al., 1969; y'Edynak, 1989; Jacobs, 1994; Fernandes et al., 2013), including dimensional similarities between Late Pleistocene and Holocene samples from southern Africa (Black, 2014).

Table 7
Comparative mandibular lateral deciduous incisor crown dimensions.

Population	*n*	x̄	SD	Reference
MD diameter				
SAM-AP 6403		**4.90 (est. 5.10)**		
Die Kelders SAM-AP 6288		5.00 (est. 5.20)		Grine (1998)
Die Kelders SAM-AP 6248		5.60 (est. 5.70)		Grine et al. (1991)
San (M + F)	57	4.53	0.40	This study
South African (M + F)	26	4.66	0.40	Grine (1986)
African American (M)	312	4.70	0.39	Anderson (2005)
African American (M)	29	4.80	0.33	Vaughn and Harris (1992)
Australian Aborigine (M)	34	5.01	0.45	Margetts and Brown (1978)
Naisoi (M)	28	4.69	0.40	Bailit et al. (1968)
European (M + F)	50	4.69	0.33	Liversidge and Molleson (1999)
European (M)	247	4.86	0.35	Seipel (1946)
European American (M)	65	4.74	0.35	Moorrees (1959)
European American (M)	69	4.58	0.43	Black (1978)
East Asian Japanese (M + F)	61	4.85	0.28	Kitagawa et al. (2002)
Neandertal (M + F)	17	5.42	0.43	This study
BL diameter				
SAM-AP 6403		**4.74**		
Die Kelders SAM-AP 6288		5.00		Grine (1998)
Die Kelders SAM-AP 6248		4.50		Grine et al. (1991)
San (M + F)	58	4.22	0.34	This study
South African (M + F)	25	4.09	0.37	Grine (1986)
Liberian (M + F)	21	4.10	0.20	Moss and Chase (1966)
Australian Aborigine (M)	33	4.75	0.35	Margetts and Brown (1978)
Naisoi (M)	26	4.26	0.39	Bailit et al. (1968)
European (M + F)	59	4.25	0.33	Liversidge and Molleson (1999)
East Asian Japanese (M + F)	65	4.32	0.28	Kitagawa et al. (2002)
Neandertal (M + F)	16	4.89	0.31	This study

Acknowledgements

We thank Sarah Wurz (formerly at the Iziko Museums of South Africa) for facilitating access to the faunal collections, which led to identification of the specimens reported here. We are grateful to Shelley L. Smith for generously providing unpublished data on pollical distal phalanx size from her dissertation. The illustrations were masterfully composed by Luci Betti-Nash. Research support to C.W. Marean was provided by National Science Foundation grants BCS-9912465 and BCS-0130713. We thank Ashley Hammond, the editor and an anonymous reviewer for useful comments on the manuscript.

References

Almécija, S., Moyà-Solà, S., Alba, D.M., 2010. Early origin for human-like precision grasping: a comparative study of pollical distal phalanges in fossil hominins. PLoS One 5, e11727.
Almécija, S., Shrewsbury, M., Rook, L., Moyà-Solà, S., 2014. The morphology of *Oreopithecus bambolii* pollical distal phalanx. Am. J. Phys. Anthropol. 153, 582–597.
Al Qahtani, S.J., Hector, M.P., Liversidge, H.M., 2010. The London atlas of human tooth development and eruption. Am. J. Phys. Anthropol. 142, 481–490.
Anderson, A., 2005. Dentition and occlusion development in African American children: mesiodistal crown diameters and tooth-size ratios of primary teeth. Ped. Dent. 27, 121–128.
Avery, G., Cruz-Uribe, K., Goldberg, P., Grine, F.E., Klein, R., Lenardi, M.J., Marean, C.W., Rink, W.J., Schwarcz, H.P., Thackeray, A.I., Wilson, M.L., 1997. The 1992–93 excavations at the Die Kelders Middle and Later Stone Age cave site, South Africa. J. Field Archaeol. 24, 263–291.
Bailit, H.L., DeWitt, S.J., Leigh, R.A., 1968. The size and morphology of the Naisoi dentition. Am. J. Phys. Anthropol. 28, 271–288.
Black, T.K., 1978. Sexual dimorphism in the tooth-crown diameters of the deciduous teeth. Am. J. Phys. Anthropol. 48, 77–82.
Black, W., 2014. Dental Morphology and Variation across Holocene Khoesan People of Southern Africa. Ph.D. Dissertation, University of Cape Town.
Brace, C.L., 1995. Trends in the evolution of human tooth size. In: Moggi-Cecchi, J. (Ed.), Aspects of Dental Biology: Palaeontology and Evolution. International Institute for the Study of Man, Florence, pp. 437–446.
Brace, C.L., Vizthum, V.J., 1984. Human tooth size at Mesolithic, Neolithic and modern levels at Niah Cave, Sarawak: comparison with Asian populations. Sarawak Mus. J. 33, 75–82.
Brace, C.L., Rosenberg, K.R., Hunt, K.D., 1987. Gradual change in human tooth size in the Late Pleistocene and post-Pleistocene. Evol. 41, 705–720.
Calcagno, J.M., 1986. Dental reduction in post-Pleistocene Nubia. Am. J. Phys. Anthropol. 70, 349–363.
Cardoso, H.F.V., Severino, R.S.S., 2010. The chronology of epiphyseal union in the hand and foot from dry bone observations. Int. J. Osteoarchaeol. 20, 737–746.
Chamla, M.C., 1980. Étude des variations métriques des couronnes dentaires du Nord-Africains de l'Épipaléolithique à l'Époque Actuelle. L'Anthropol. 84, 254–271.
Christensen, A.F., 1998. Odontometric microevolution in the Valley of Oaxaca, Mexico. J. Hum. Evol. 34, 333–360.
Conard, N.J., 2008. A critical view of the evidence for a southern African origin of behavioral modernity. S. Afr. Archaeol. Soc. Goodwin Ser. 10, 175–179.
Crevecoeur, I., 2002. Étude morphologique et biométrique des ossements de mains retrouvés dans la couche Castelperronienne du gisement de Saint-Césaire (Charente-Maritime). D.E.A. d'Anthropologie Biologique, Université de Bordeaux 1.
Crevecoeur, I., 2008. Étude Anthropologique du Squelette du Paléolithique Supérieur de Nazlet Khater 2 (Égypte). Leuven University Press, Leuven.
Deacon, H.J., 1992. Southern Africa and modern human origins. Phil. Trans. Roy. Soc. Lond. B 337, 177–183.
Deacon, H.J., 2001. Modern human emergence: an African archaeological perspective. In: Tobias, P.V., Raath, M.A., Moggi-Cecchi, J., Doyle, G.A. (Eds.), Humanity from African Naissance to Coming Millennia: Colloquia in Human Biology and Palaeoanthropology. University of Florence Press, Florence, pp. 217–226.
du Plessis, A., le Roux, S.G., Guelpa, A., 2016. The CT scanner facility at Stellenbosch University: an open access X-ray computed tomography laboratory. Nucl. Instrum. Methods Phys. Res. B 384, 42–49.
Feathers, J.K., Bush, D.A., 2000. Luminescence dating of the Middle Stone Age deposits at Die Kelders. J. Hum. Evol. 38, 91–119.
Federative Committee on Anatomical Terminology, 1998. Terminologia Anatomica: International Anatomical Terminology. Thieme, New York.
Fernandes, D.M., Silva, A.M., O'Donnabhain, B., Pinhasi, R., 2013. Dental microevolution in Portuguese Neolithic and modern samples using an alternative morphometric analysis. Anthropol. Sci. 121, 25–30.
Flecker, H., 1932. Roentgenographic observations of the times of appearance of epiphyses and their fusion with the diaphyses. J. Anat. 67, 118–164.
Frayer, D., 1977. Metric dental change in the European Upper Paleolithic and Mesolithic. Am. J. Phys. Anthropol. 46, 109–120.
Garn, S.M., Lewis, A.B., Walcnga, A.J., 1969. Crown-size profile patterns and presumed evolutionary trends. Am. Anthropol. 71, 79–84.
Glisanz, V., Ratib, O., 2005. Hand Bone Age. A Digital Atlas of Skeletal Maturity. Springer, New York.
Grine, F.E., 1986. Anthropological aspects of the deciduous teeth of South African blacks. In: Singer, R., Lundy, J.K. (Eds.), Variation, Culture and Evolution in African Populations: Papers in Honour of Professor Hertha de Villiers. Witwatersrand University Press, Johannesburg, pp. 47–83.
Grine, F.E., 1990. Deciduous dental features of Kalahari San: comparison of non-metrical traits. In: Sperber, G.H. (Ed.), From Apes to Ancestors. Wiley-Liss, New York, pp. 153–169.

Grine, F.E., 1998. Additional human fossils from the Middle Stone Age of Die Kelders Cave 1, South Africa: 1995 excavation. S. Afr. J. Sci. 94, 229–235.
Grine, F.E., 2000. Middle Stone Age human fossils from Die Kelders Cave 1, Western Cape Province, South Africa. J. Hum. Evol. 38, 129–145.
Grine, F.E., 2005. Enamel thickness of deciduous and permanent molars in modern *Homo sapiens*. Am. J. Phys. Anthropol. 126, 14–31.
Grine, F.E., 2016. The late quaternary hominins of Africa: the skeletal evidence from MIS 6-2. In: Jones, S.C., Stewart, B.A. (Eds.), Africa from MIS 6-2: Population Dynamics and Paleoenvironments. Springer, Dordrecht, pp. 323–381.
Grine, F.E., Klein, R.G., 1985. Pleistocene and Holocene human remains from Equus Cave, South Africa. Anthropol. 8, 55–98.
Grine, F.E., Klein, R.G., Volman, T.P., 1991. Dating, archaeology and human fossils from the Middle Stone Age Layers of Die Kelders Cave 1, South Africa. J. Hum. Evol. 21, 363–395.
Grine, F.E., Wurz, S., Marean, C.W., 2017. The Middle Stone Age human fossil record from Klasies River Main Site. J. Hum. Evol. 103, 53–78.
Henshilwood, C.S., Marean, C.W., 2003. The origin of modern human behavior. Critique of the models and their test implications. Curr. Anthropol. 44, 627–637.
Henshilwood, C., d'Errico, F., Yates, R., Jacobs, Z., Tribolo, C., Duller, G.A.T., Mercier, N., Sealy, J.C., Valladas, H., Watts, I., Wintle, A.G., 2002. Emergence of modern human behaviour: Middle Stone Age engravings from South Africa. Science 295, 1278–1280.
Henshilwood, C.S., d'Errico, F., van Niekerk, K.L., Coquinot, Y., Jacobs, Z., Lauritzen, S.E., Menu, M., García-Moreno, R., 2011. A 100,000-year-old ochre-processing workshop at Blombos Cave, South Africa. Science 334, 219–222.
Hill, M.K., 2004. Dental reduction and diet in the prehistoric Ohio River valley. Dent. Anthropol. 17, 34–44.
International Anatomical Nomenclature Committee, 1989. Nomina Anatomica, 6th ed. Churchill Livingstone, Edinburgh.
Jacobs, K., 1994. Human dento-gnathic metric variation in Mesolithic/Neolithic Ukraine: possible evidence of demic diffusion in the Dnieper Rapids region. Am. J. Phys. Anthropol. 95, 1–26.
Joseph, J., 1951. The sesamoid bones of the hand and the time of fusion of the epiphyses of the thumb. J. Anat. 85, 221–229.
Jungers, W.L., Falsetti, A.B., Wall, C.E., 1995. Shape, relative size, and size-adjustments in morphometrics. Yearb. Phys. Anthropol. 38, 137–161.
Kitagawa, Y., Manabe, Y., Oyamada, J., Rokutanda, A., 2002. Japanese deciduous tooth size: past and present. Anthropol. Sci. 110, 335–347.
Kivell, T.L., Deane, A.S., Tocheri, M.W., Orr, C.M., Schmid, P., Hawks, J., Berger, L.R., Churchill, S.E., 2015. The hand of *Homo naledi*. Nat. Commun. 6, 8431.
Klein, R.G., 2001. Southern Africa and modern human origins. J. Anthropol. Res. 57, 1–16.
Klein, R.G., Cruz-Uribe, K., 2000. Middle and Later Stone Age large mammal and tortoise remains from Die Kelders Cave 1, Western Cape Province, South Africa. J. Hum. Evol. 38, 169–195.
Klein, R.G., Avery, G., Cruz-Uribe, K., Halkett, D.J., Parkington, J.E., Steele, T., Volman, T.P., Yates, R., 2004. The Ysterfontein 1 Middle Stone Age site, South Africa, and early human exploitation of coastal resources. Proc. Nat. Acad. Sci. 101, 5708–5715.
Lacy, S.A., 2014. Periodontal disease and health in western Eurasian Late Pleistocene humans. Am. J. Phys. Anthropol. 153(S58), 163.
Liversidge, H.M., Molleson, T.I., 1999. Deciduous tooth size and morphogenetic fields in children from Christ Church, Spitalfields. Archs. Oral Biol. 44, 7–13.
Lorenzo, C., 2007. Evolución de la mano en los homínidos. Análisis morfológico de los fósiles de la Sierra de Atapuerca. Ph.D. Dissertation, Universidad Complutense de Madrid.
Marean, C.W., 2015. An evolutionary anthropological perspective on modern human origins. Ann. Rev. Anthropol. 44, 533–556.
Marean, C.W., Goldberg, P., Avery, G., Grine, F.E., Klein, R.G., 2000. Middle Stone Age stratigraphy and excavations at Die Kelders Cave 1 (Western Cape Province, South Africa): the 1992, 1993, and 1995 field seasons. J. Hum. Evol. 38, 7–42.
Marean, C.W., Bar-Matthews, M., Bernatchez, J., Fisher, E., Goldberg, P., Herries, A.I., Jacobs, Z., Jerardino, A., Karkanas, P., Minichillo, T., Nilssen, P.J., Thompson, E., Watts, I., Williams, H.M., 2007. Early human use of marine resources and pigment in South Africa during the Middle Pleistocene. Nature 449, 905–908.
Margetts, B., Brown, T., 1978. Crown diameters of the deciduous teeth in Australian aboriginals. Am. J. Phys. Anthropol. 48, 493–502.
Margvelashvili, A., Zollikofer, C.P.E., Lordkipanidze, D., Tafforeau, P., Ponce de León, M.S., 2016. Comparative analysis of dentognathic pathologies in the Dmanisi mandibles. Am. J. Phys. Anthropol. 160, 229–253.
Matiegka, J., 1938. *Homo předmostensis*. Fosilní člověk z Předmostí na Moravě II. Ostatní Části Kostrové. Česká Akademie Věd a Umění, Prague.
McCown, T.D., Keith, A., 1939. The Stone Age of Mount Carmel II: The Fossil Human Remains from the Levalloiso-Mousterian. Clarendon Press, Oxford.
McCrossin, M.L., 1992. Human molars from later Pleistocene deposits of Witkrans Cave, Gaap Escarpment, Kalahari margin. Hum. Evol. 7, 1–10.
Mittra, E.S., Smith, H.F., Lemelin, P., Jungers, W.L., 2007. Comparative morphometrics of the primate apical tuft. Am. J. Phys. Anthropol. 134, 449–459.
Moorrees, C.F.A., 1959. The Dentition of the Growing Child. A Longitudinal Study of Dental Development Between 3 and 18 Years of Age. Harvard University Press, Cambridge.
Moss, M.L., Chase, P.S., 1966. Morphology of the Liberian Negro deciduous teeth. I. Odontometry. Am. J. Phys. Anthropol. 24, 215–230.
Musgrave, J.H., 1970. An anatomical study of the hands of Pleistocene and recent man. Ph.D. Dissertation, University of Cambridge.
Musgrave, J.H., 1973. The phalanges of Neanderthal and Upper Palaeolithic hands. In: Day, M.H. (Ed.), Human Evolution. Taylor and Francis, London, pp. 59–85.
Napier, J.R., 1962. Fossil hand bones from Olduvai Gorge. Nature 196, 409–411.
Niewoehner, W.A., 2007. Neanderthal hands in their proper perspective. In: Harvati, K., Harrison, T. (Eds.), Neandertals Revisited: New Approaches and Perspectives. Springer, New York, pp. 157–190.
Philstrom, B.L., Michalowicz, B.S., Johnson, N.W., 2005. Periodontal diseases. Lancet 366, 1809–1820.
Pinhasi, R., Meiklejohn, C., 2011. Dental reduction and the transition to agriculture in Europe. In: Pinhasi, R., Stock, J.T. (Eds.), Human Bioarchaeology of the Transition to Agriculture. Wiley, Chichester, pp. 451–474.
Pinhasi, R., Eshed, V., Shaw, P., 2008. Evolutionary changes in the masticatory complex following the transition to farming in the southern Levant. Am. J. Phys. Anthropol. 135, 136–148.
Pyle, S.I., Waterhouse, A.M., Greulich, W.W., 1971. A Radiographic Standard of Reference for the Growing Hand and Wrist. Case Western Reserve University Press, Cleveland.
R Core Team, 2014. R: A Language and Environment for Statistical Computing, 3.1.2. R Foundation for Statistical Computing. http://www.r-project.org.
Rightmire, G.P., Deacon, H.J., 1991. Comparative studies of Late Pleistocene human remains from Klasies River Mouth, South Africa. J. Hum. Evol. 20, 131–156.
Rosas, A., 1985. Falanges humanas de la Sima des los Huesos (Cueva Mayor), Sierra de Atapuerca (Burgos). Estudio anatomico y comparativo. Actas Cong. Esp. Antropol. Biol. 4, 557–566.
Schwarcz, H.P., Rink, W.J., 2000. ESR dating of the Die Kelders Cave 1 site, South Africa. J. Hum. Evol. 38, 121–128.
Schweitzer, F.R., 1970. A preliminary report of excavations of a cave at Die Kelders. S. Afr. Archaeol. Bull. 25, 136–138.
Schweitzer, F.R., 1979. Excavations at Die Kelders, Cape Province, South Africa: the Holocene deposits. Ann. S. Afr. Mus. 78, 101–233.
Seipel, C., 1946. Variation in tooth position: a metric study of variation and adaptation in the deciduous and permanent dentitions. Swedish Dent. J. 39, 1–176.
Shrewsbury, M.M., Johnson, R.K., 1983. Form, function and evolution of the distal phalanx. J. Hand Surg. 8, 475–479.
Shrewsbury, M.M., Marzke, M.W., Linscheid, R.L., Reece, S.P., 2003. Comparative morphology of the pollical distal phalanx. Am. J. Phys. Anthropol. 121, 30–47.
Singer, R., Wymer, J., 1982. The Middle Stone Age at Klasies River Mouth in South Africa. University of Chicago Press, Chicago.
Smith, S.L., 2000. Shape variation of the human pollical distal phalanx and metacarpal. Am. J. Phys. Anthropol. 113, 329–348.
So, L.L.Y., 1997. Skeletal maturation of the hand and wrist and its correlation with dental development. Aust. Orthod. J. 15, 1–9.
Stack, H.G., 1958. Some details of the anatomy of the terminal segment of the finger. Acta Orthop. Belg. 24, 113–116.
Susman, R.L., 1989. New hominid fossils from the Swartkrans Formation (1979–1986) excavations: postcranial specimens. Am. J. Phys. Anthropol. 79, 451–474.
Susman, R.L., 1998. Hand function and tool behavior in early hominids. J. Hum. Evol. 35, 23–46.
Susman, R.L., Creel, N., 1979. Functional and morphological affinities of the subadult hand (OH7) from Olduvai Gorge. Am. J. Phys. Anthropol. 51, 311–332.
Tankard, A.J., 1976. The stratigraphy of a coastal cave and its palaeoclimatic significance. Palaeoecol. Afr. 9, 151–159.
Tankard, A.J., Schweitzer, F.R., 1974. The geology of Die Kelders Cave and environs: a palaeoenvironmental study. S. Afr. J. Sci. 70, 365–369.
Tankard, A.J., Schweitzer, F.R., 1976. Textural analysis of cave sediments: Die Kelders, Cape Province, South Africa. In: Davidson, D.A., Shackley, M.L. (Eds.), Geoarchaeology. Duckworth, London, pp. 289–316.
Texier, P.J., Porraz, G., Parkington, J., Rigaud, J.P., Poggenpoel, C., Miller, C., Tribolo, C., Cartwright, C., Coudenneau, A., Klein, R., Steele, T., Verna, C., 2010. A Howiesons Poort tradition of engraving ostrich eggshell containers dated to 60,000 years ago at Diepkloof Rock Shelter, South Africa. Proc. Natl. Acad. Sci. 107, 6180–6185.
Trinkaus, E., 1983. The Shanidar Neandertals. Academic Press, New York.
Trinkaus, E., 2006. Modern human versus Neandertal evolutionary distinctiveness. Curr. Anthropol 47, 597–620.
Trinkaus, E., 2016. The evolution of the hand in Pleistocene *Homo*. Anatomical, developmental, functional and paleontological evidence. In: Kivel, T., Lemelin, P., Richmond, B.G., Schmitt, D. (Eds.), The Evolution of the Primate Hand. Springer, New York, pp. 545–571.
Trinkaus, E., Haduch, E., Valde-Nowak, P.W., Wojtal, P., 2014. The Obłazowa 1 early modern human pollical phalanx and Late Pleistocene distal thumb proportions. Homo 65, 1–12.
Vanhaeren, M., d'Errico, F., van Niekerk, K.L., Henshilwood, C.S., Erasmus, R.M., 2013. Thinking strings: additional evidence for personal ornament use in the Middle Stone Age at Blombos Cave, South Africa. J. Hum. Evol. 64, 500–517.
Vaughn, M.D., Harris, H., 1992. Deciduous tooth size standards for American blacks. J. Tenn. Dent. Assoc. 72, 30–33.
Verneau, R., 1906. Les Grottes de Grimaldi (Baoussé-Roussé), Tome II – Fascicule I. Anthropologie. Imprimérie de Monaco, Monaco.
Wadley, L., Hodgskiss, T., Grant, M., 2009. Implications for complex cognition from the hafting of tools with compound adhesives in the Middle Stone Age, South Africa. Proc. Nat. Acad. Sci. 106, 9590–9594.
Wurz, S., 2008. Modern behavior at Klasies River. S. Afr. Archaeol. Soc. Goodwin Series 10, 150–156.
y'Edynak, G., 1989. Yugoslav Mesolithic dental reduction. Am. J. Phys. Anthropol. 78, 17–36.